Letter

Band-Pass Sampling in High-Order BOC Signal Acquisition

Zhijun Liu [ID], Baiyu Li *, Xiangwei Zhu, Lixun Li and Guangfu Sun

College of Electronic Science, National University of Defense Technology, Changsha 410073, China;
liuzhijun1988@sina.cn (Z.L.); zhuxiangwei@nudt.edu.cn (X.Z.); lilixun1985@163.com (L.L.);
gfsunmail@163.com (G.S.)
* Correspondence: leehenry0505@126.com; Tel.: +86-151-1624-5810

check for updates

Abstract: The binary offset carrier (BOC) modulation, which has been adopted in modern global navigation satellite systems (GNSS), provides a higher spectral compatibility with BPSK signals, and better tracking performance. However, the autocorrelation function (ACF) of BOC signals has multiple peaks. This feature complicates the acquisition process, since a smaller time searching step is required, which results in longer searching time or greater amounts of hardware resources. Another problem is the high Nyquist frequency, which leads to high computational complexity and power consumption. In this paper, to overcome these drawbacks, the band-pass sampling technique for multiple signals is introduced to BOC signals. The sampling frequency can be reduced significantly. Furthermore, the ACF of the sampled signal has only two secondary peaks, so that the code phase can be searched with a larger searching step. An acquisition structure base on dual-loop is proposed, to completely eliminate the ambiguity and compensate the subcarrier Doppler. The acquisition performance and the computational complexity are also analysed.

1. Introduction

The BOC modulation has been adopted in modernized global positioning system (GPS), European Galileo project, and China's BeiDou-3. BOC signals are characterised by a rectangular subcarrier, which split the signal spectrum around two main lobes at $\pm f_{\text{sc}}$, the subcarrier repetition frequency. It can improve the tracking performance, and enhance spectrum compatibility due to the narrow ACF, and split spectrum [1]. More detail and characteristics of BOC modulation can be found in literature [2–5].

However, the acquisition process of BOC signals becomes more complex, due to the multiple peaks in the ACF envelope, which requires a large number of timing hypotheses to search a given uncertainty window [6]. Thus the acquisition becomes more computationally expensive and time consuming. Another problem in BOC acquisition is the high Nyquist sampling frequency [7], which increases the computational burden and power consumption.

Some techniques have been reported to remove the impact of the secondary peaks in the ACF. The subcarrier phase cancellation technique (SPCT) [8] introduces a quadrature squared subcarrier, called QBOC, to eliminate the ambiguity problem. In the autocorrelation side-peak cancellation technique (ASPeCT) proposed in [9], subtraction of the cross-correlation between the BOC and PRN signals from the BOC autocorrelation is employed; but the technique is applicable only to sine-BOC(n,n). The Pseudo-Correlation Function (PCF) [10] method constructs a single-peak ACF using a special designed reference signal. However, it will suffer from severe detection performance degradation for

high-order BOC signal. The techniques mentioned above can remove the impact of the secondary peaks in the ACF, but they all process the upper and lower sidebands together, resulting in a high sampling frequency and computational complexity.

The main idea behind the BPSK-like method is that the BOC signal can be obtained as the sum of two BPSK signals, located at positive and negative sub-carrier frequencies. The effect of sub-carrier modulation can be removed by using a pair of single-sideband correlators. A receiver may use a single-side band (SSB), either the upper or lower sidebands, or use dual-side band (DSB), where both bands are combined non-coherently. Due to filtering and correlation losses, the BPSK-like methods bring some degradation. The losses are 3dB for SSB and about 0.5 dB for DSB [11]. However, the BPSK-like method needs two RF channels, mixers and analog-to-digital converters (ADC), which increase the implementation complexity [11].

In this paper, the band-pass sampling technique [12–16] is introduced in BOC signal sampling to remove the secondary peaks, as well as to reduce the sampling frequency. Band-pass sampling is the technique of under-sampling a band-pass signal to achieve a frequency translation via intentional aliasing [17]. If the sampling frequency is f_s, then the spectrum of the sampled signal can be obtained by replicating the spectrum of the original signal at multiples of f_s [18]. Since a BOC signal can be treated as the sum of two BPSK signals with adjacent center frequencies [19], the band-pass sampling technique for multiple signals [14,17,20] can be used. Furthermore, taking into account the subcarrier Doppler, a dual-loop based acquisition structure is proposed to acquire the sampled signal.

The remainder of this paper is organized as follows. Section 2 introduces the dual-sideband model of BOC signals, which is the basis of band-pass sampling; in Section 3, the band-pass sampling is applied and the sampling parameters are derived. The dual-loop based acquisition structure is also described in detail. The detection probability and computational complexity are analysed in Section 4. The conclusions are drawn in Section 5.

2. Dual-Sideband Model of BOC Signals

The BOC(*m,n*) signal can be expressed as:

$$s(t) = Ad(t)c(t)sc(t)\cos(2\pi f_0 t + \theta_0) \tag{1}$$

where A is the signal amplitude; $d(t)$ is the navigation data; $c(t)$ is the pseudorandom noise (PN) code with code rate $f_c = m \times 1.023$ MHz; $sc(t)$ is the squared subcarrier with frequency $f_{sc} = n \times 1.023$ MHz; f_0 and θ_0 are the carrier frequency and phase, respectively. Generally, the integration period is shorter than the bit duration. So we will ignore the navigation data, that is, $d(t) \equiv 1$.

The squared-wave subcarrier can be expanded in Fourier series [19] (for sine-phased BOC signals):

$$sc(t) = \sum_{i=1}^{\infty} a_i \sin(2\pi i f_{sc} t) \tag{2}$$

where $a_i = \frac{1}{T_{sc}} \int_0^{T_{sc}} sc(t) \cdot \sin(2\pi i f_{sc} t) dt$ is the Fourier coefficients; $T_{sc} = 1/f_{sc}$ is the subcarrier period.

Equation (2) indicates that the squared-wave subcarrier can be expressed as the sum of a series of sine waves. In practice, both the transmitter and the receiver are band-limited, which means that the high-frequency component of the signals will be filtered out. So in band-limited cases, the squared-wave subcarrier can be approximated by:

$$sc(t) \approx \sum_{i=1}^{N} a_i \sin(2\pi i f_{sc} t) \tag{3}$$

where N is the number of terms preserved by front-end filtering.

For high-order BOC signals, the front-end filter may remove all the harmonic waves. Then the subcarrier can be approximated by a sine wave:

$$sc(t) \approx a_1 \sin(2\pi i f_{sc} t) \tag{4}$$

As a result, the BOC(*m*,*n*) signal can be approximated by

$$
\begin{aligned}
s(t) & \approx A a_1 c(t) \sin(2\pi f_{sc} t) \cos(2\pi f_0 t + \theta_0) \\
& = \frac{A a_1}{2} c(t) \sin(2\pi (f_0 + f_{sc})t + \theta_0) - \frac{A a_1}{2} c(t) \sin(2\pi (f_0 - f_{sc})t + \theta_0)
\end{aligned}
\tag{5}
$$

Equation (5) indicates that in band-limited cases, high-order BOC signals can be treated as a dual-sideband signal.

3. BOC Acquisition Based on Band-Pass Sampling

3.1. Problems in BOC Acquisition

As a result of the subcarrier, the ACF of BOC signals has multiple peaks. The squared magnitude ACF is directly relevant to the class of non-coherent energy detection acquisition receivers considered here. Figure 1a illustrates the normalized squared magnitude ACFs of BOC(15,2.5) and BPSK(2.5). As shown in this figure, the squared magnitude ACFs of BOC(15,2.5) has as many as 23 peaks, while BPSK(2.5) has a unique peak.
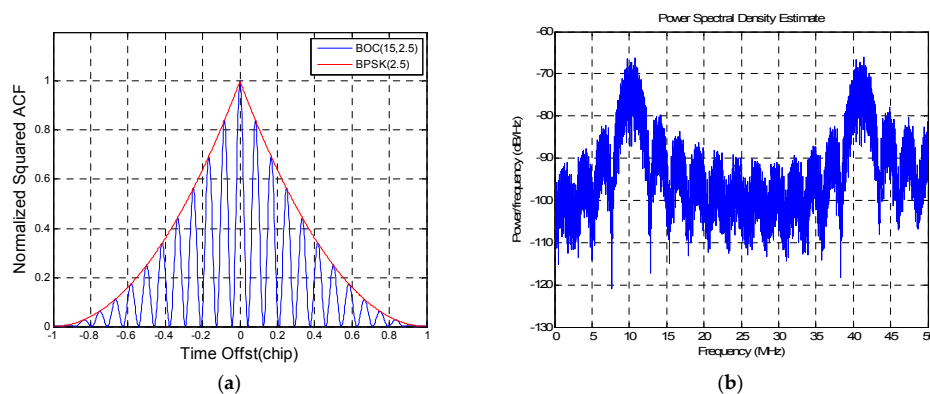
Figure 1. The normalized squared ACF and power spectrum density. (**a**) Squared ACFs; (**b**) Power spectrum density of BOC(15,2.5).

This indicates that the step of the searching time bin should be sufficiently small to be able to detect the main peak of the ACF (i.e., we need a higher number of timing hypotheses in order to search a given time-uncertainty window compared to BPSK case) [6]. Another problem is that the bandwidth of BOC(*m*,*n*) signals is much wider than BPSK(*n*) signals, so that the Nyquist frequency is very high, which results in a higher computational complexity.

3.2. Band-Pass Sampling Technique

As mentioned before, the secondary peaks and the high sampling frequency of high-order BOC signals result in high complexity. Band-pass sampling technique can be used to remove the secondary peaks and reduce computational complexity.

For a single-band signal, the range of f_s is given by [12]:

$$\frac{2 f_U}{n} \leq f_s \leq \frac{2 f_L}{n-1} \tag{6}$$

where f_L and f_U are the lower and upper frequencies, respectively; *n* is an positive integer.

The frequency of the sampled signal is [17]:

$$f'_{IF} = \begin{cases} \text{rem}(f_{IF}, f_s), & \text{fix}\left(\frac{f_{IF}}{f_s/2}\right) \text{ is even} \\ f_s - \text{rem}(f_{IF}, f_s), & \text{fix}\left(\frac{f_{IF}}{f_s/2}\right) \text{ is odd} \end{cases} \tag{7}$$

where f_{IF} is the intermediate frequency of the continuous signal; fix(a) is the truncated portion of argument a and rem(a,b) is the remainder after division of a by b.

For a dual-sideband signal, the range of f_s is:

$$f_s \in \left[\frac{2f_{U1}}{n_1}, \frac{2f_{L1}}{n_1 - 1}\right] \cap \left[\frac{2f_{U2}}{n_2}, \frac{2f_{L2}}{n_2 - 1}\right] \tag{8}$$

The signal bands must not overlap in the frequency spectrum of the resultant sampled bandwidth. This can be expressed mathematically for two signals as [17]:

$$\left|f'_{IF1} - f'_{IF2}\right| > \frac{B_1 + B_2}{2} \tag{9}$$

where f'_{IF1} and f'_{IF2} are the center frequencies of the sampled signals; B_1 and B_2 are the bandwidth of the two signals, respectively.

3.3. Band-Pass Sampling for High-Order BOC Signals

Since the filtered high-order BOC signal can be treated as a dual-sideband signal, the band-pass sampling technique can be applied. In this study, the signal will be sampled at intermediate frequencies, and the intermediate frequency is an important parameter.

If the intermediate frequency of BOC(m,n) is f_{IF}, then the center frequencies of the two sidebands are:

$$f_1 = f_{IF} - f_{sc}$$
$$f_2 = f_{IF} + f_{sc}$$

Define $p_1 = \text{fix}\left(\frac{f_1}{f_s/2}\right)$ and $p_2 = \text{fix}\left(\frac{f_2}{f_s/2}\right)$. To simplify the analysis, we choose the sampling frequency f_s to make sure p_2 is even. Then the spectrum transition will be discussed for two cases.

Case a: p_1 is odd.

In this case, the frequencies of the sampled signals are:

$$\begin{cases} f'_1 = (1 + k_1)f_s - f_1 \\ f'_2 = f_2 - k_2 f_s \end{cases} \tag{10}$$

where $k_1 = \text{fix}(f_1/f_s)$ and $k_2 = \text{fix}(f_2/f_s)$.

The spectrum transition is depicted in Figure 2. Since the signal is real, there is always a negative spectrum.
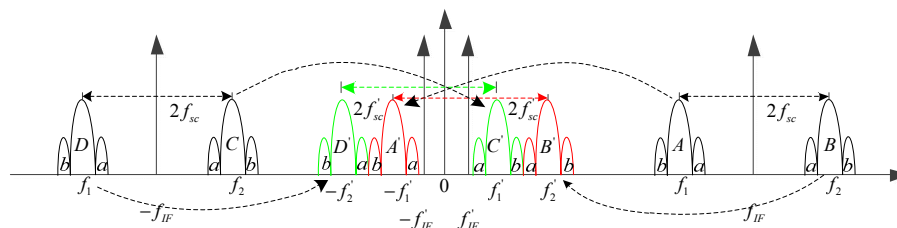
Figure 2. Spectrum transition where p_1 is odd.

As shown in Figure 2, the spectrum marked C' is actually from C, and it is an inverse version of A. So, if we treat A' and B' as the target sampled signal, then C' and D' are the negative spectrum. For the sake of clarity, we will change the sign of f_1, then (10) should be rewritten as:

$$
\begin{cases}
f_1' = f_1 - (1 + k_1) f_s \\
f_2' = f_2 - k_2 f_s
\end{cases}
\tag{11}
$$

Case b: p_1 is even.

In this case, the frequencies of the sampled signals are:

$$
\begin{cases}
f_1' = f_1 - k_1 f_s \\
f_2' = f_2 - k_2 f_s
\end{cases}
\tag{12}
$$

The spectrum transition is depicted in Figure 3.
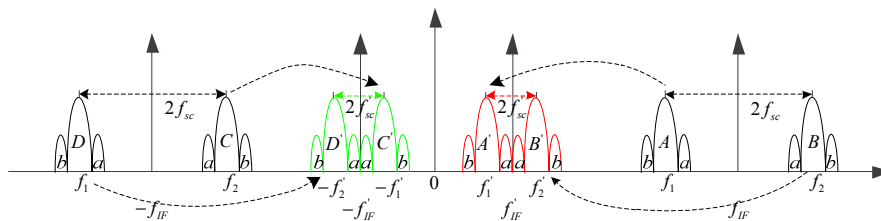
Figure 3. Spectrum transition where p_1 is even.

In summary, the frequencies of the sampled signals are:

$$
\begin{cases}
f_1' = f_1 - k_1 f_s \\
f_2' = f_2 - k_2 f_s
\end{cases}
\tag{13}
$$

where $k_2 = \text{fix}(f_2 / f_s)$ and:

$$
k_1 =
\begin{cases}
\text{fix}(f_1 / f_s) + 1 & p_1 \quad \text{is odd} \\
\text{fix}(f_1 / f_s) & p_1 \quad \text{is even}
\end{cases}
$$

Consequently, given the center frequencies of sampled sidebands, the sampling frequency and the intermediate frequency can be determined as follows:

$$
\begin{cases}
f_{IF}' - f_{sc}' = f_1 - k_1 f_s \\
f_{IF}' + f_{sc}' = f_2 - k_2 f_s \\
f_s > 2B
\end{cases}
\tag{14}
$$

where $2 f_{sc}'$ is the distance between the two sidebands of the sampled signal; $f_{IF}' = (f_1' + f_2')/2$ is the intermediate frequency of the sampled signal; B is the bandwidth of either sideband.

Equation (14) can be simplified as:

$$
\begin{cases}
f_s = 2 \frac{f_{sc} - f_{sc}'}{k_2 - k_1} \\
f_s > 2B \\
f_{IF} = f_{IF}' + \frac{k_1 + k_2}{2} f_s
\end{cases}
\tag{15}
$$

The sampling frequency must also satisfy (8).

Taking Galileo E1 PRS signal (BOC(15,2.5) modulated) as an example, Figure 4 illustrates the power spectrum density (PSD) and the ACF of the sampled signal ($f_{sc}' = 2.5575\,\text{MHz}, f_{IF}' = 0$).

The sampling frequency and the intermediate frequency are $f_s = 12.7875\,\text{MHz}$ and $f_{IF} = 25.575\,\text{MHz}$, respectively.
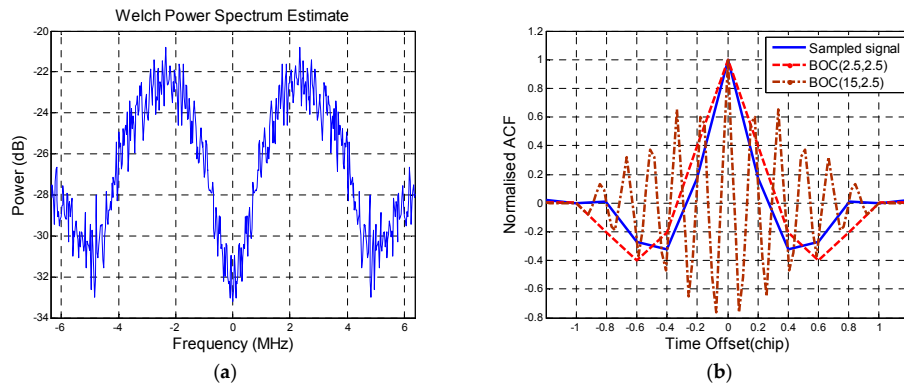
Figure 4. PSD (power spectrum density) and ACF (autocorrelation function) of the sample d BOC (binary offset carrier) signals. (**a**) PSD; (**b**) ACF.

Figure 4 shows that the PSD and ACF of the sampled signal are similar to that of a BOC(*n,n*) signal and the number of the remaining secondary peaks is reduced to 2, much less than that of BOC(15,2.5).

3.4. Acquisition of Band-Pass Sampled BOC Signals

Taking the velocity into consideration, the sampled signal can be expressed as:

$$s_{BS}(nT_s) = Aa_1 \cdot c(nT_s) \sin\left[2\pi\left(f'_{sc} + f_{dsc}\right)nT_s\right] \cos\left[2\pi\left(f'_{IF} + f_d\right)nT_s + \theta_0\right] \tag{16}$$

where f_d is carrier Doppler; f_{dsc} is subcarrier Doppler; T_s is the sampling interval.

Given v as the relative speed between the satellite and the receiver, the Doppler frequencies of the lower band and upper band are:

$$f_{dL} = -\tfrac{v}{c}(f_0 - f_{sc})$$
$$f_{dU} = -\tfrac{v}{c}(f_0 + f_{sc})$$

Then the Doppler frequencies of the carrier and subcarrier are:

$$f_d = \tfrac{f_{dL} + f_{dU}}{2} = -\tfrac{v}{c}f_0$$
$$f_{dsc} = \tfrac{f_{dU} - f_{dL}}{2} = -\tfrac{v}{c}f_{sc}$$

Equation (16) shows that the sampled signal is still a BOC signal, with subcarrier frequency f'_{sc} and intermediate frequency f'_{IF}.

In the acquisition process, the receiver must determine the carrier frequency offset, the subcarrier frequency offset and the time offset. Then the acquisition turns into a 3-dimensional searching process. However, since the ratio between f_d and f_{dsc} always equals the ratio between f_0 and f_{sc}; that is, $f_d/f_{dsc} = f_0/f_{sc}$, the acquisition is actually a 2-dimensional searching process.

An acquisition structure based on dual-loop is proposed in Figure 5.
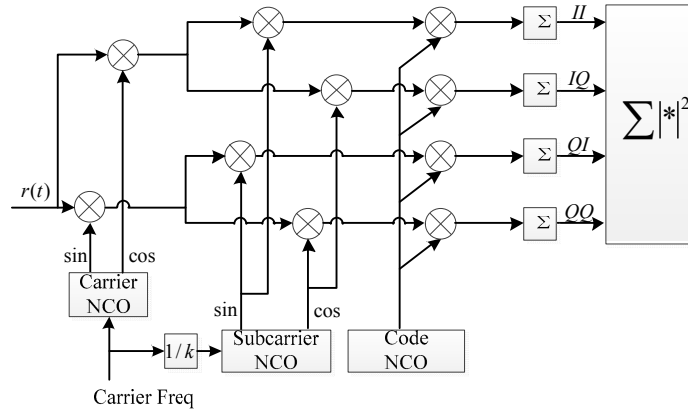
Figure 5. Dual-loop based acquisition structure.

In Figure 5, $k = f_d / f_{dsc} = f_0 / f_{sc}$. The correlators' outputs are:

$$
\begin{aligned}
II &= \frac{A a_1}{N} \sum_{n=0}^{N-1} s_{BS}(nT_s) c(nT_s - \varepsilon) \cos\left(2\pi \hat{f}_{IF} nT_s + \hat{\theta}_0\right) \sin\left(2\pi \hat{f}_{sc} nT_s + \hat{\theta}_{sc}\right) \\
&= \frac{A a_1}{4N} \sum_{n=0}^{N-1} c(nT_s) c(nT_s - \varepsilon) \cos(2\pi \Delta f_{dsc} t + \Delta \theta_{sc}) \cdot \cos(2\pi \Delta f_d t + \Delta \theta_0) \\
&\approx \widetilde{R}(\varepsilon, \Delta f_{dsc}, \Delta f_d) \cos[\pi \Delta f_{dsc}(N-1)T_s + \Delta \theta_{sc}] \cos[\pi \Delta f_d(N-1)T_s + \Delta \theta_0] + Z_{II} \\
IQ &\approx \widetilde{R}(\varepsilon, \Delta f_{dsc}, \Delta f_d) \sin[\pi \Delta f_{dsc}(N-1)T_s + \Delta \theta_{sc}] \cos[\pi \Delta f_d(N-1)T_s + \Delta \theta_0] + Z_{IQ} \\
QI &\approx \widetilde{R}(\varepsilon, \Delta f_{dsc}, \Delta f_d) \cos[\pi \Delta f_{dsc}(N-1)T_s + \Delta \theta_{sc}] \sin[\pi \Delta f_d(N-1)T_s + \Delta \theta_0] + Z_{QI} \\
QQ &\approx \widetilde{R}(\varepsilon, \Delta f_{dsc}, \Delta f_d) \sin[\pi \Delta f_{dsc}(N-1)T_s + \Delta \theta_{sc}] \sin[\pi \Delta f_d(N-1)T_s + \Delta \theta_0] + Z_{QQ}
\end{aligned}
\tag{17}
$$

where $\widetilde{R}(\varepsilon, \Delta f_{dsc}, \Delta f_d) = \frac{A a_1}{4} R(\varepsilon) \frac{\sin(\pi \Delta f_{dsc} N T_s)}{N \sin(\pi \Delta f_{dsc} T_s)} \frac{\sin(\pi \Delta f_d N T_s)}{N \sin(\pi \Delta f_d T_s)}$; $R(\varepsilon)$ is the ACF of the PN-code; ε is the time offset; $\hat{f}_{sc}$ and $\hat{f}_{IF}$ are the frequencies of the subcarrier numerically controlled oscillator (NCO) and carrier NCO; $\hat{\theta}_{sc}$ and $\hat{\theta}_0$ are the phases of the subcarrier NCO and carrier NCO; Δf_{dsc} and Δf_d are the Doppler errors of the subcarrier and carrier; $\Delta \theta_{sc}$ and $\Delta \theta_0$ are the phase errors of the subcarrier and carrier; Z_{II}, Z_{IQ}, Z_{QI}, Z_{QQ} are independent zero-mean Gaussian variables.

Then the decision statistic is given by:

$$
X = II^2 + IQ^2 + QI^2 + QQ^2
\tag{18}
$$

4. Performance Analysis

In this section, we will analyse the detection performance and the computational complexity.

4.1. Detection Probability

With the presence of a signal, the decision statistic X in (18) is a non-central χ^2 random variable with $\nu = 4$ degrees of freedom and the non-central parameter $\lambda = \left| \widetilde{R}(\varepsilon, \Delta f_{dsc}, \Delta f_d) \right|^2$. Its probability density function (PDF) is given by $p(x) = 1/2\sqrt{x/\lambda}\, e^{-1/2(x+\lambda)} I_1(\sqrt{\lambda x})$. Given the detection threshold η, the detection probability can be expressed in terms of the generalized Marcum Q-function $Q_M(\alpha, \beta)$ [21] as $P_d = Q_1\left(\sqrt{\lambda}, \sqrt{\eta} \right)$.

Figure 6 depicts the detection probabilities of the proposed method, dual-side band method, and the match filter method. For the proposed method, the sampling frequency and the intermediate frequency are $f_s = 12.7875\,\text{MHz}$ and $f_{IF} = 25.575\,\text{MHz}$, respectively. The integration period is 1 ms.
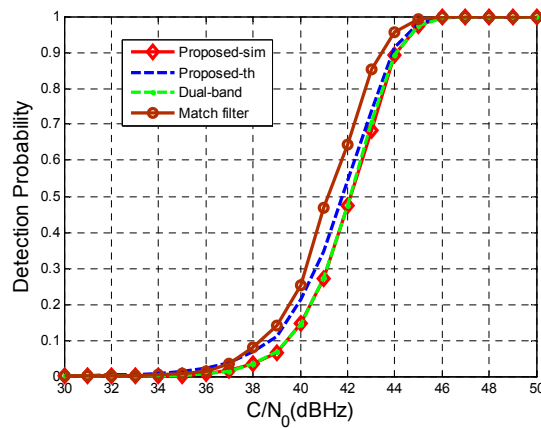
Figure 6. Detection probabilities of different methods.

Figure 6 shows that match filter method outperforms the other two methods, and the performance of the proposed method and dual-side band method is nearly the same.

Figure 7 illustrates the detection probability under different sampling frequencies and intermediate frequencies, which are listed in Table 1.
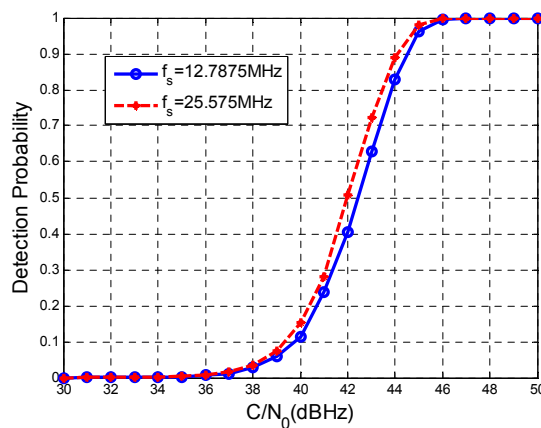
Figure 7. Detection probabilities with different sampling frequencies.

Table 1. Sampling frequencies and intermediate frequencies.

No.	k_2	k_1	f_{IF} (MHz)	f_s (MHz)
1	2	1	38.3625	25.575
2	3	1	25.575	12.7875

Figure 7 shows that the detection performance suffers from a slight degradation with a lower sampling frequency. The reason is that more signal component is filtered out.

4.2. Computational Complexity

We use the number of computations required for the acquisition process to assess the computational complexity.

The samples of the received signals are cross-correlated against a stored reference PN-code. These cross-correlations are repeated with the lag between the received signal and the stored reference successively incremented, until the decision statistic exceeds a threshold, at which time a verification test is performed. If the latter test is passed, the initial acquisition process is complete.

If the sampling frequency is f_s, the number of multiplies and adds required for each cross-correlation is $T_p f_s$, where T_p is the code period. If the time searching step is δt, then for a given initial time uncertainty, the number of the total computation is:

$$N_{tot} = T_p f_s \cdot \frac{\Delta t}{\delta t} \tag{19}$$

The time searching step is typically chosen to be one-half the distance between the correlation peak and its first zero value [6]. So for BOC(m,n), the time searching step is $\delta t_1 = Tc/2$ for the proposed method and dual-side band method, and $\delta t_2 = nT_c/(4m)$ for match filer method, where $Tc = 1/f_c$ is the PN-code chip duration.

We take BOC(15,2.5) as an example to show the computational complexity of the proposed method, dual-side band method, and match filter method. The results are list in Table 2.

Table 2. Computational complexity.

	Proposed	**Dual-Side Band**	**Match Filter**
f_s	12.7875 MHz	12.7875 MHz	71.61 MHz
Complexity	$\frac{2\Delta t \cdot T_p}{T_c} \times 12.7875 \times 10^6$	$\frac{2\Delta t \cdot T_p}{T_c} \times 12.7875 \times 10^6$	$\frac{4m\Delta t \cdot T_p}{nT_c} \times 71.61 \times 10^6$
Ratio against proposed	1	1	67.2

Table 2 shows that the computations required for match filter method is 67.2 times the proposed method. The result also indicates that if processors with the same speed grade are used, the proposed method and dual-side band method need much less time to acquire the signal.

4.3. An Experiment

In this subsection, we tried to acquire BOC(15,2.5). The signal parameters are: $C/N_0 = 45$ dBHz, $f_d = 2$ kHz, $f_{dsc} = 19.5$ Hz. The sampling frequency and the intermediate frequency are $f_s = 12.7875$ MHz and $f_{IF} = 25.575$ MHz, respectively. The integration period is 1 ms. Figure 8 shows the 2-dimensional search results obtained by the proposed method. On account of the strong signal strength, the correct peak is easy to identify, which demonstrates the feasibility of the proposed algorithm.
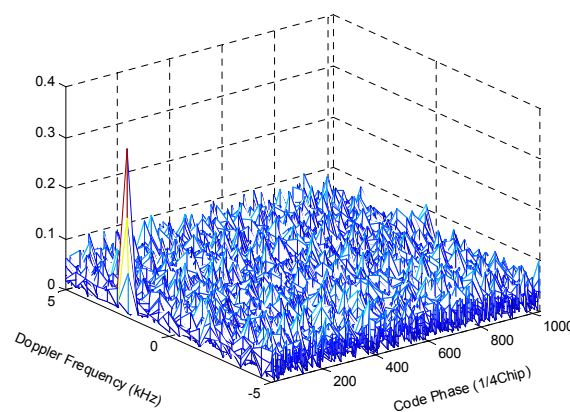
Figure 8. Frequency and time search results for BOC(15,2.5).

5. Conclusions

In this paper, the band-pass sampling technique for multiple signals is introduced to BOC signals to reduce the computational complexity. Using this technique, the sampling frequency is reduced significantly and only two secondary peaks remain in the ACF of the sampled signal. An acquisition

method based on dual-loop structure is also proposed to remove the ambiguity completely and to compensate the subcarrier Doppler. The detection probability and computational complexity are analysed. The detection performance of the proposed method degrades a little compared to the match filter method, but nearly the same as DSB method. The computational complexity is assessed by the number of multiplies and adds required for the acquisition process. When the sampling frequency is 12.7875 MHz, the multiplies and adds required are 1/67.2 of the match filter method.

References

1. Betz, J.W. Binary offset carrier modulations for radio navigation. *Navigation* **2001**, *48*, 227–246. [CrossRef]
2. Chronopoulos, S.K.; Koliopanos, C.; Pappa, A.; Angelis, C.T. Simulation of a Feasible Galileo System Operating in L1 and E5 Bands. In *Lecture Notes of the Institute for Computer Sciences, Social Informatics and Telecommunications Engineering*; Springer: Berlin/Heidelberg, Germany, 2010; Volume 43, Chapter 3; pp. 35–43.
3. Lohan, E.S.; Lakhzouri, A.; Renfors, M. Binary-offset-carrier modulation techniques with applications in satellite navigation systems. *Wirel. Commun. Mob. Comput.* **2010**, *7*, 767–779. [CrossRef]
4. Rebeyrol, E.; Macabiau, C.; Lestarquit, L.; Ries, L.; Issler, J.L.; Boucheret, M.L.; Bousquet, M. BOC Power Spectrum Densities. In Proceedings of the ION NTM 2005, San Diego, CA, USA, 24–26 January 2005; pp. 769–778.
5. Pratt, A.R.; Owen, J. BOC Modulations Waveform. In Proceedings of the ION GPS/GNSS, Portland, OR, USA, 23–25 June 2003; pp. 1044–1057.
6. Fishman, P.; Betz, J.W. Predicting Performance of Direct Acquisition for the M-Code Signal. In Proceedings of the ION NMT 2000, Anaheim, CA, USA, 26–28 January 2000; pp. 574–582.
7. Feng, T. Decimation double-phase estimator: An efficient and unambiguous high-order binary offset carrier tracking algorithm. *IEEE Signal Process. Lett.* **2016**, *23*, 905–909. [CrossRef]
8. Ward, P.W. A Design Technique to Remove the Correlation Ambiguity in Binary Offset Carrier (BOC) Spread Spectrum Signals. In Proceedings of the ION NTM 2004, San Diego, CA, USA, 26–28 January 2004; pp. 886–896.
9. Julien, O.; Macabiau, C.; Cannon, M.E.; Lachapelle, G. ASPeCT: Unambiguous sine-BOC(n,n) acquisition/tracking technique for navigation applications. *IEEE Trans. Aerosp. Electron. Syst.* **2007**, *43*, 150–162. [CrossRef]
10. Yao, Z.; Cui, X.; Lu, M.; Feng, Z.; Yang, J. Pseudo-correlation-function-based unambiguous tracking technique for sine-BOC signals. *IEEE Trans. Aerosp. Electron. Syst.* **2010**, *46*, 1782–1796. [CrossRef]
11. Burian, A.; Lohan, E.S.; Renfors, M. BPSK-Like Methods for Hybrid Search Acquisition of Galileo Signals. In Proceedings of the IEEE International Conference on Communications, Istanbul, Turkey, 11–15 June 2006.
12. Vaughan, R.G.; Scott, N.L.; White, D.R. The theory of bandpass sampling. *IEEE Trans. Signal Process.* **1991**, *39*, 1973–1984. [CrossRef]
13. Brown, J.L., Jr. On quadrature sampling of bandpass signals. *IEEE Trans. Aerosp. Electron. Syst.* **1979**, *AES-15*, 366–371. [CrossRef]
14. Figueiras-Vidal, A.R. Sampling bandpass signals. *IEEE Trans. Aerosp. Electron. Syst.* **1981**, *AES-17*, 288–295. [CrossRef]
15. Waters, W.M.; Jarrett, B.R. Bandpass signal sampling and coherent detection. *IEEE Trans. Aerosp. Electron. Syst.* **1982**, *AES-18*, 731–736. [CrossRef]
16. Qi, R.; Coakley, F.P.; Evans, F.G. Practical consideration for bandpass sampling. *Electron. Lett.* **1996**, *32*, 1861–1862. [CrossRef]
17. Akos, D.M.; Stockmaster, M.; Tsui, B.Y.; Casschera, J. Direct bandpass sampling of multiple distinct RF signals. *IEEE Trans. Commun.* **1999**, *47*, 983–988. [CrossRef]
18. Liu, J.C. Bandpass Sampling of Multiple Single Sideband RF Signals. In Proceedings of the 2008 3rd International Symposium on Communications, St Julians, Malta, 12–14 March 2008; pp. 863–866. [CrossRef]

19. Borio, D. Double phase estimator: New unambiguous binary offset carrier tracking algorithm. *IET Radar Sonar Navig.* **2014**, *8*, 729–741. [CrossRef]

20. Bae, J.; Park, J. An efficient algorithm for bandpass signals of multiple signals. *IEEE Signal Process. Lett.* **2006**, *13*, 193–196. [CrossRef]

21. Proakis, J.G. *Digital Communications*; McGrawHill: New York, NY, USA, 1995.